

# Three-dimensional Digital Mapping of the Noboribetsu Geothermal Field, Kuttara Volcano, Hokkaido, Japan, using a Helicopter-borne High-resolution Laser Scanner

Yoshihiko GOTO\*, Satoru MATSUZUKA\*\* and Seiji KAMEYAMA\*\*

(Received February 9, 2011; Accepted August 26, 2011)

An aerial high-resolution laser-scanner survey was performed in November 2006 over the Noboribetsu Geothermal Field on Kuttara Volcano, Hokkaido, Japan. The 2×2.4 km survey area covers the entire geothermal field. A three-dimensional digital map, produced from the laser-scanning data, shows detailed topographic features of the geothermal field. Notable features include a cryptodome formed by the intrusion of high-viscosity magma, a plain that is inferred to have formed by river damming due to growth of the cryptodome, and explosion craters that are aligned NW–SE. These features suggest that the geothermal field has evolved by complex volcanic activity and ground deformation involving cryptodome growth, river damming, and phreatic explosions. The NW–SE elongation of the cryptodome and the NW–SE alignment of explosion craters indicate the injection of magma and hydrothermal fluids along NW–SE-trending fractures. High-resolution laser-scanner surveys provide valuable information for understanding the geology of geothermal fields.

**Key words:** laser scanner, digital mapping, three dimensions, explosion crater, Noboribetsu Geothermal Field, Kuttara Volcano

## 1. Introduction

LIDER (light detection and ranging) is a powerful tool for studying the morphological features of volcanoes (e.g., Hunter *et al.*, 2003; Chiba *et al.*, 2007a, 2007b; Pesci *et al.*, 2007). Three-dimensional digital mapping based on high-resolution laser-scanning data provides invaluable information on the distribution and morphology of craters, lavas, domes, and pyroclastic deposits, as well as reworked deposits. Laser-scanner mapping is particularly useful for surveying topographic features in thickly vegetated areas, for which “tree-removing” data filtering can be used to reveal the topography of the ground surface.

We performed an aerial laser-scanner survey over the Noboribetsu Geothermal Field at Kuttara Volcano, Hokkaido, Japan, using a high-resolution laser scanner mounted on a manned helicopter. The Noboribetsu Geothermal Field is covered with thick vegetation, and three-dimensional digital mapping based on the laser-scanning data provided an excellent tool with which to study detailed topographic features of the geothermal field, as a basis for understanding its geology. This paper describes the topographic features of the geothermal

field and discusses the characteristics of volcanic activity in the field.

## 2. Noboribetsu Geothermal Field

The Noboribetsu Geothermal Field lies in the western part of Kuttara Volcano (Fig. 1), an andesitic to rhyolitic composite volcano (elevation, 549 m above sea level) with a small caldera at its summit (Lake Kuttara). The volcano evolved over the period 80–45 ka, involving early silicic explosive activity and subsequent strato-volcano building associated with caldera collapse at 40 ka (Katsui *et al.*, 1988; Yamagata, 1994; Moriizumi, 1998; Moriya, 2003). The geothermal field, which is inferred to have formed after the collapse of the caldera (Katsui *et al.*, 1988), is approximately 1 km wide (NE–SW) and 1.5 km long (NW–SE), and is situated at an altitude of 200–370 m. It is one of the major geothermal fields in Japan.

The geothermal field is characterized by a dacitic cryptodome (Hiyoriyama Cryptodome), a volcanic lake (Oyunuma Lake), and a fumarolic valley (Jigokudani Valley) (Fig. 1). The Hiyoriyama Cryptodome, in the northern part of the geothermal field, rises 377 m above

\*College of Environmental Technology, Graduate School of Engineering, Muroran Institute of Technology, Mizumoto-cho 27-1, Muroran, Hokkaido 050-8585, Japan.

\*\*Tanaka Consultant Co., Ltd, Shinkai-cho 2-1-3,

Tomakomai, Hokkaido 050-8585, Japan.

Corresponding author: Yoshihiko Goto  
e-mail: ygoto@mmm.muroran-it.ac.jp

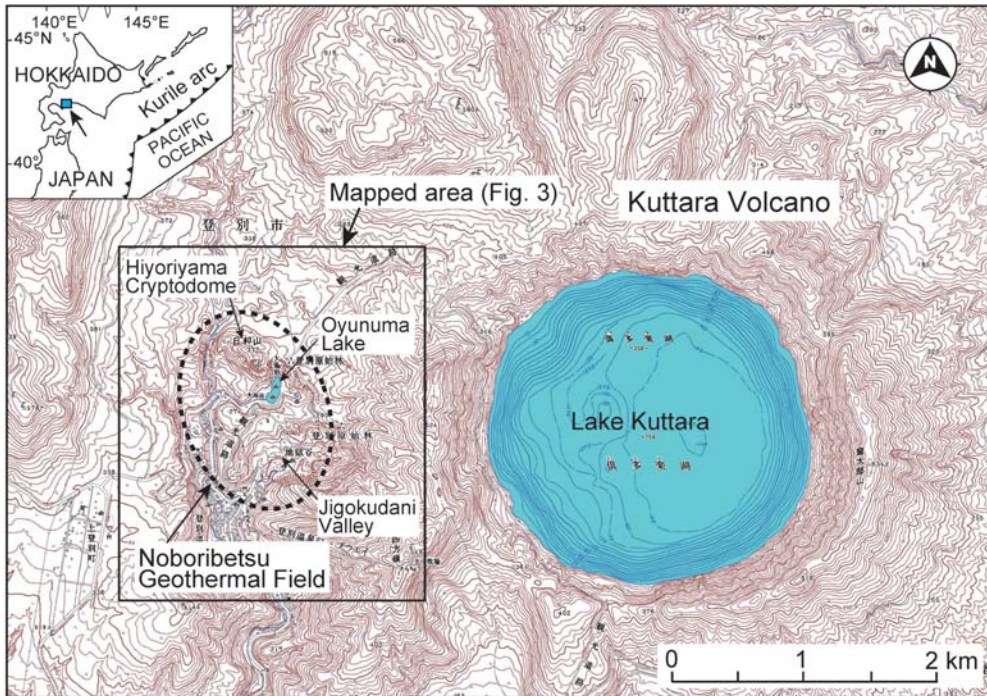


Fig. 1. Location map of the Noboribetsu Geothermal Field at Kuttara Volcano, Hokkaido, Japan. The survey area (Fig. 3) is shown by the rectangle. The contour interval on the base map is 10 m.

sea level and has active fumaroles at its summit. Oyunuma Lake, in the central part of the geothermal field, is 115 × 210 m in surface area and is filled with hot acidic water. The Jigokudani Valley, in the southern part of the geothermal field, extends for 500 m ENE–WSW and hosts a number of active fumaroles. The geothermal field is widely covered with thick vegetation, mainly broadleaf trees.

### 3. Laser-scanner survey

The laser-scanner survey covered the entire Noboribetsu Geothermal Field, encompassing an area extending 2 km E–W and 2.4 km N–S (Fig. 1). The survey was carried out by Tanaka Consultant Co. Ltd using a Develo LISA3 instrument (Fig. 2). Under typical conditions, the scanner is able to measure distances of up to 1000 m with an accuracy of  $\pm 10$  mm (Table 1). The lightweight instrument can be mounted on an airplane, a manned helicopter, or a radio-controlled helicopter. In the present survey, LISA3 was mounted on a manned Robinson R44 helicopter (Fig. 2A).

The survey was performed on 25 November 2006. Considerations for setting the date of the survey were (1) the timing of the end of leaf fall to minimize tree noise, (2) the number of available GPS NAVSTAR satellites (to minimize positioning error), (3) good flight conditions, and (4) good ground conditions with-

out snowfall. On 25 November, the broadleaf trees in the survey area were bare, the weather was fine and calm, and there was no snow on the ground.

The flight height of the helicopter was 250–300 m above the ground, and the measuring time was 1.5 h (10:00–11:30 AM local time). The position of the helicopter was recorded at 1-s intervals using a Global Positioning System (GPS) and at 0.01-s intervals using an inertial measurement unit (IMU). After the flight, the three-dimensional flight route was reconstructed from the GPS and IMU data.

The laser-scanning data were initially cleaned to remove noise and then filtered to produce a digital terrain model (DTM), which shows the bare ground surface. As part of the filtering process, trees and buildings were carefully removed using the application TerraScan (Terrasolid Co. Ltd). Both automatic and handpicking methods were used in this process to avoid removing necessary information. After filtering, a triangulated irregular network (TIN) was produced from the ground data. In turn, a three-dimensional digital map was produced from the TIN, using the Red Relief Image Map technique (Chiba *et al.*, 2007a) (Fig. 3). The colors in the map express the angle of inclination of the ground surface (expressed by the saturation of red, whereby steep slopes appear highly saturated) and the opening ratio (Yokoyama *et al.*, 1999) of the ground

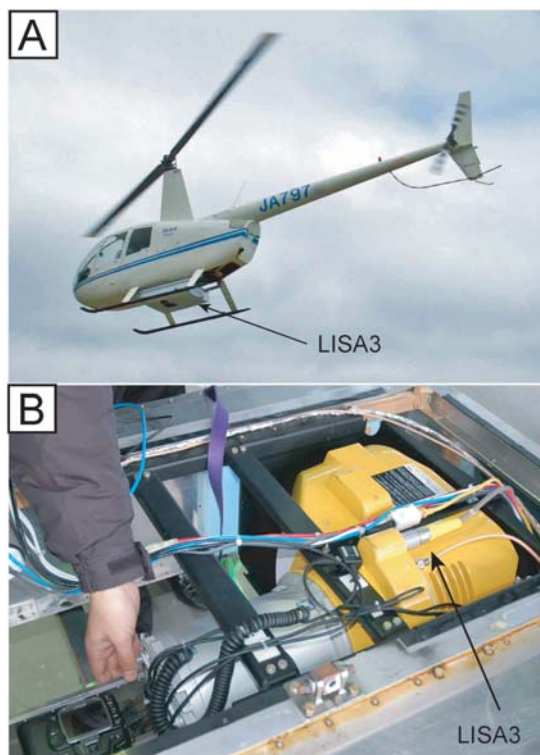


Fig. 2. (A) Photograph of the LISA3 instrument mounted on a manned helicopter. (B) Close-up photograph of the LISA3 instrument.

surface (expressed by the brightness of red, whereby ridges appear bright red and valleys appear dark red).

#### 4. Results

Figure 3 shows the obtained three-dimensional digital map of the Noboribetsu Geothermal Field; an annotated version is shown in Figure 4. The notable topographic features in the map are an elongate cryptodome oriented NW–SE (Hiyoriyama Cryptodome), a plain located northeast of the cryptodome (Hiyoriyama Plain), and explosion craters aligned NW–SE (Fig. 4). These features and their interpretations are described in detail in the following sections.

##### 4-1 Hiyoriyama Cryptodome

The Hiyoriyama Cryptodome is elongate NW–SE and ranges in diameter from 350 to 550 m (Fig. 4). It rises 130 m above the surrounding area, with its highest point being 377 m above sea level. Figure 5A and 5B shows bird's eye (oblique), three-dimensional images of the cryptodome from different viewpoints. The cryptodome has a pyramidal form (Fig. 5A), suggesting it formed by the intrusion of high-viscosity magma. The cryptodome consists of dacite containing 70 wt.% SiO<sub>2</sub> (Goto and Danhara, 2011), which is consistent with its

Table 1. Specifications of the laser scanner, Develo LISA3. The laser class is based on the safety classification of laser devices according to Japan Industrial Standard (JIS) C6802. Note that beam divergence of the LISA3 is 0.25 mrad (i.e., a beam diameter of 25 mm at a distance of 100 m).

Model	Develo LISA3
Laser class	Class 1
Measuring distance	Maximum 1000 m Minimum 2 m
Accuracy	±10 mm
Measuring rate	8333 points/second
Laser frequency	Near-infrared light
Beam divergence	0.25 mrad
Scanning range	80° (vertical), 360° (horizontal)
Line number	1-20/second
Weight	25 kg (without battery)

pyramidal form. The surface of the cryptodome is moderately eroded (Fig. 5A), indicating a relatively old age of formation. Field surveys revealed that the surface of the cryptodome is covered with tall trees and short bamboo forest. The cryptodome has been dated as  $15 \pm 4$  ka and  $14 \pm 4$  ka by the fission-track method (Goto and Danhara, 2011), which is consistent with the moderately eroded topography and thick vegetation cover. The NW–SE elongation of the cryptodome (Fig. 4) suggests that the feeder dyke beneath the dome also strikes NW–SE.

On the northern slope of the dome, a curved ridge extends for more than 300 m (Fig. 5B). The ridge rises to 330–340 m above sea level and protrudes 5–10 m above the slope, forming a V-shaped valley on its uphill side. The ridge is hidden by thick vegetation and is identified here for the first time. Field surveys revealed that the ridge and the V-shaped valley form a conspicuous step on the slope, although they are covered with tall trees and short bamboo forest. The ridge may have formed by the fracturing and detachment of surficial sediment, or the northward displacement of the sediment during growth of the cryptodome.

The cryptodome has several explosion craters on its surface (Figs. 4 and 5A). These craters are inferred to have formed by phreatic explosions that occurred after emplacement of the dome. The explosion crater at the summit (the Hiyoriyama Summit Crater; no. 3 in Fig. 5A) is elongate NW–SE and ranges in diameter from 40 to 95 m. The crater retains its primary morphological features, including the crater rim and wall, and it contains active fumaroles. Field surveys (Goto *et al.*, 2011) found that a phreatic deposit erupted from the crater overlies the Us-b tephra (Yokoyama *et al.*, 1973; Machida and Arai, 2003), which was emplaced in AD 1663. The Hiyoriyama Summit Crater is thus inferred

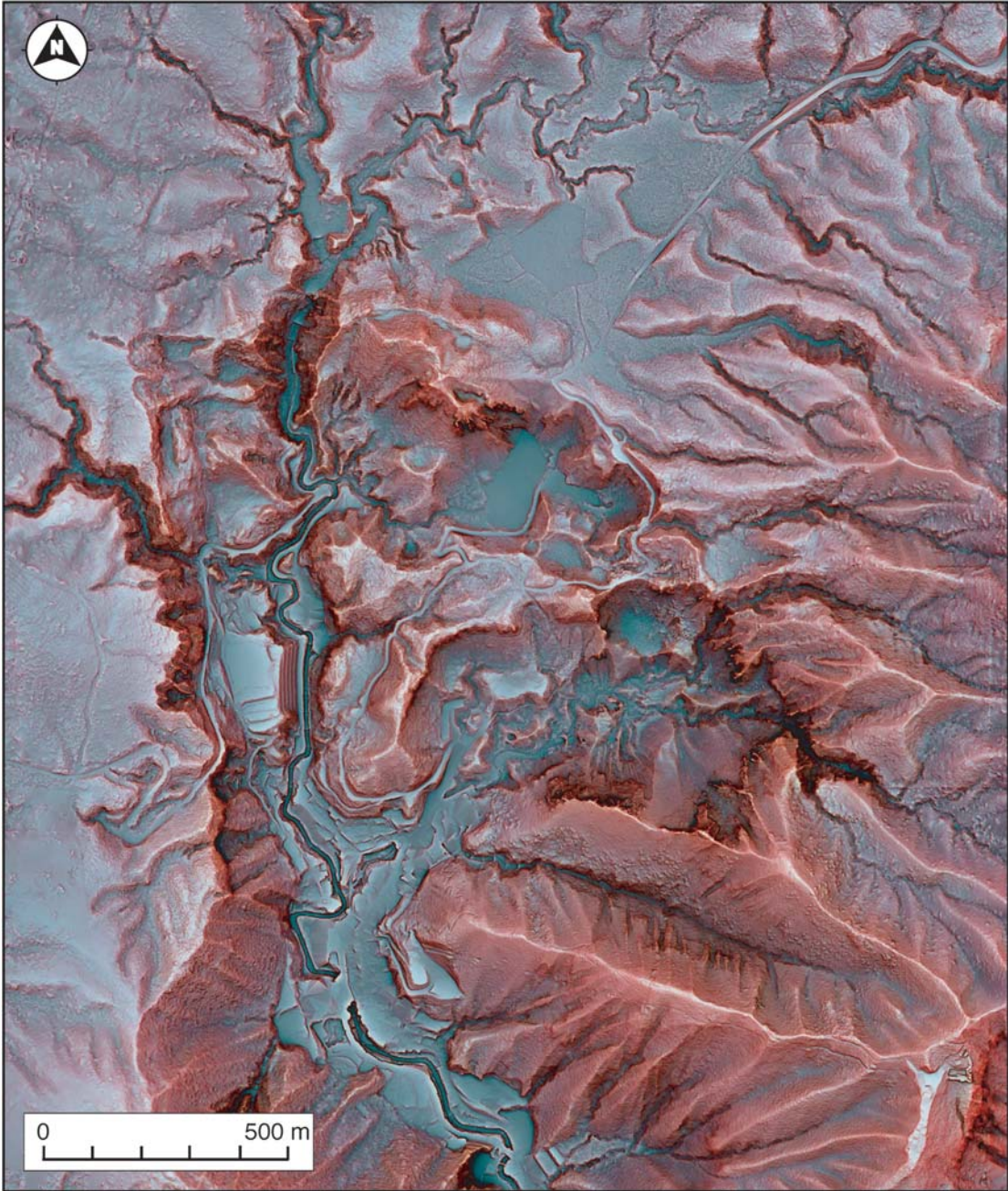


Fig. 3. Three-dimensional digital map of the Noboribetsu Geothermal Field, expressed using the Red Relief Image Map technique.

to have formed after AD 1663. The well-preserved morphology of the crater is consistent with the stratigraphy of the deposit. Three explosion craters on the slope of the dome, named Hiyoriyama North, Hiyoriyama Southwest, and Hiyoriyama South (nos. 4, 5, and 6, respectively, in Fig. 5A and Table 2), are circular in

plan view and have diameters of 35, 115, and 75 m, respectively. These craters are more strongly eroded than the Hiyoriyama Summit Crater, possibly indicating they are relatively old. Field surveys revealed that these craters contain no active fumaroles.

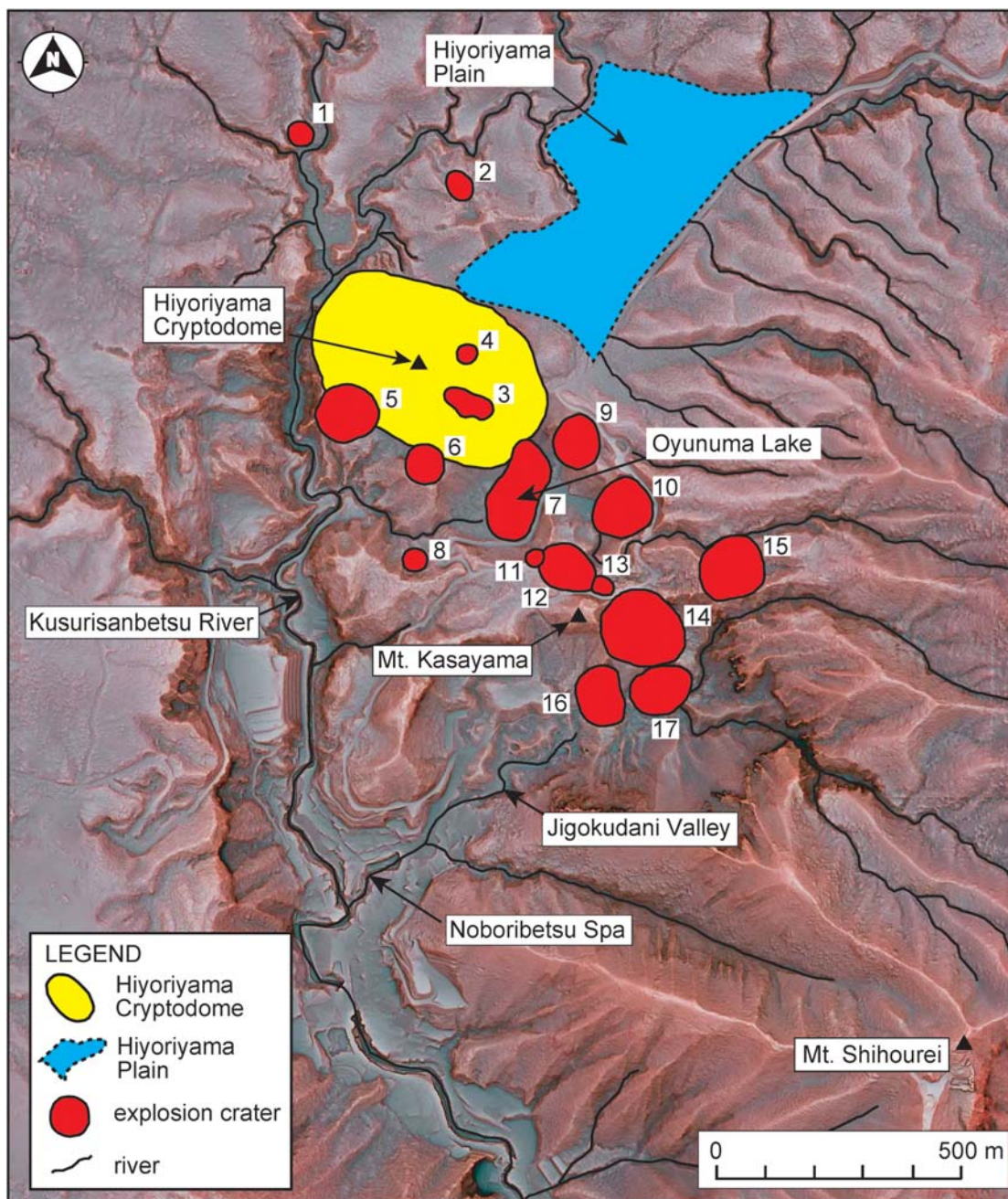


Fig. 4. Interpretation of the map shown in Fig. 3. The names and dimensions of the numbered craters are listed in Table 2.

#### 4-2 Hiyoriyama Plain

The Hiyoriyama Plain occurs northeast of the Hiyoriyama Cryptodome (Figs. 4 and 5B). The plain is semi-rectangular in plan view, being 300 m (NW–SE)–800 m (NE–SW) in size, and is located at 300 m above sea level. Its flat topography is conspicuous in the

rugged terrain of the region. East of the plain, the river system trends E–W, whereas within the plain the pre-existing river system is buried by sediment (Figs. 3 and 4). The southwestern termination of the plain is sharply defined by the Hiyoriyama Cryptodome (Fig. 5 B). Field surveys suggest that the plain is a dried

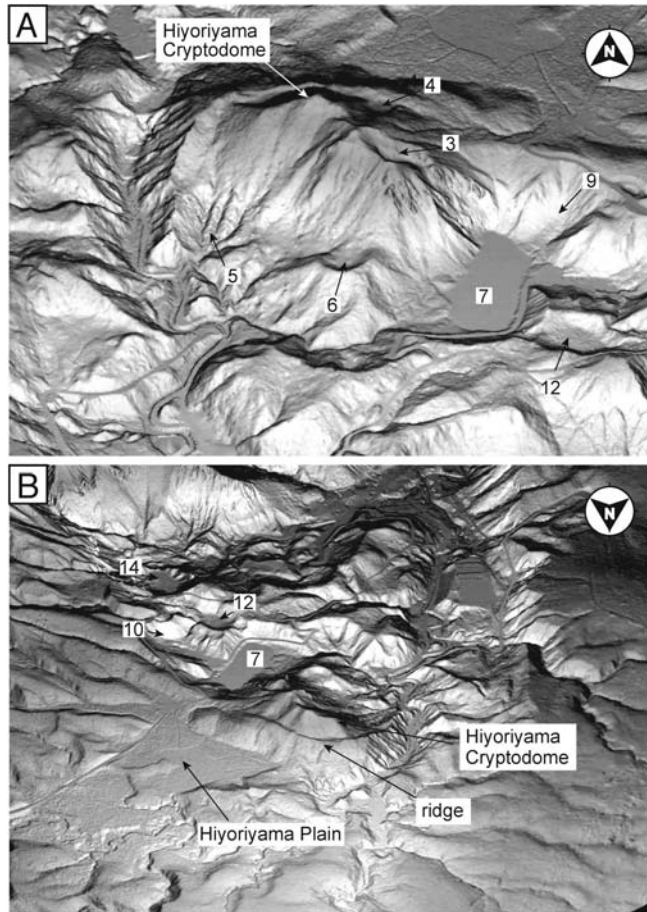


Fig. 5. (A) Bird's eye (oblique), three-dimensional image of the Hiyoriyama Cryptodome viewed from the south. Crater numbers correspond to those in Fig. 4 and Table 2. The Hiyoriyama Cryptodome has explosion craters at its summit (crater 3) and on its slope (craters 4, 5, and 6). (B) Bird's eye (oblique), three-dimensional image of the Hiyoriyama Cryptodome and surrounding area viewed from the north. The cryptodome has a curved ridge on its northern slope. Hiyoriyama Plain is conspicuous in the rugged terrain of the region, and is inferred to have formed by damming of a river due to growth of the Hiyoriyama Cryptodome. Crater numbers correspond to those in Fig. 4 and Table 2.

wetland which is now covered by short bamboo and grasses. There are no lakes or ponds upon the plain.

The Hiyoriyama Plain buries the pre-existing river-influenced topography (Figs. 4 and 5B), suggesting that it formed by damming of the river and deposition of sediment behind the dam. The river system of the surrounding area indicates that the sediments were derived from rivers draining to the west. The western margin of the plain is marked by the Hiyoriyama Cryptodome, suggesting that formation of the cryptodome resulted in damming of the river, and that the dammed lake became filled with sediment. Drilling in the western part of the Hiyoriyama Plain (unpublished data) has revealed a 15-m-thick layer of peat beneath the plain. The damming

of a river due to cryptodome growth has also been reported for the 1944 eruptions at Usu volcano, Hokkaido, Japan, where the Shinzan-numa Pond formed due to growth of the Showa-shinzan Cryptodome (Mimatsu, 1995).

#### 4-3 Explosion craters

At least 17 explosion craters are identified from the map of the Noboribetsu Geothermal Field (Fig. 4), recognized by their conical morphology, circular or semicircular outline, and flat bottom. The explosion craters are 25–210 m in diameter and 5–50 m deep. The names and dimensions of the craters are listed in Table 2. Most show well-preserved primary morphology, although some are eroded. The craters are dis-

Table 2. Topographic data of explosion craters in the Noboribetsu Geothermal Field. Locations are shown in Fig. 4.

No.	Name	Shape	Diameter (m)	Depth (m)	Notes
1	Kusurisanbetsu	circular	55	10	
2	Kitanuma	semicircular	50-55	10	lake
3	Hiyoriyama Summit	semicircular	40-95	20	fumarole
4	Hiyoriyama North	circular	35	5	
5	Hiyoriyama Southwest	circular	115	10	
6	Hiyoriyama South	circular	75	10	
7	Oyunuma	semicircular	115-210	30	lake, hot spring
8	Taisho-jigoku	circular	35	20	lake, hot spring
9	Oyunuma East	circular	100	40	
10	Okunoyu	circular	115	50	lake, hot spring
11	Kasayama Northwest	circular	25	5	fumarole
12	Kasayama North	semicircular	95-115	20	
13	Kasayama Northeast	circular	25	20	
14	Senjojiki	circular	160	50	fumarole
15	Higashizawa	circular	135	20	
16	Tessen-ike	circular	120	20	hot spring
17	Urajigoku	semicircular	100-120	20	



Fig. 6. Photograph of a newly identified explosion crater (Kitanuma) in the northwestern part of the Noboribetsu Geothermal Field (crater 2 in Fig. 4). The crater is 50–55 m across; the pond within the crater is 24 m across and 2 m deep.

tributed in a NW–SE-trending zone that is 500 m wide and 1,500 m long, which also includes the Hiyoriyama Cryptodome (Fig. 4).

The three-dimensional map is useful in identifying explosion craters hidden by thick vegetation; indeed, several explosion craters were newly found by this mapping survey. For example, Kitanuma Crater (50–55 m across; no. 2 in Fig. 4) is hidden by tall trees and thick bamboo but is obvious on the three-dimensional map (Fig. 3). A field survey revealed that the crater contains a pond with fresh water (Fig. 6). Higashizawa Crater (135 m across; no. 15 in Fig. 4) is also hidden by

thick vegetation but is easily identified on the three-dimensional map (Fig. 3).

The explosion craters in the Noboribetsu Geothermal Field are relatively small (diameters of 25–210 m; Table 2), suggesting that most of them formed by phreatic explosions. Based on the degree of erosion, most of the craters are inferred to have formed during the past several thousand years. The craters show varying degrees of erosion, indicating they formed at different times, although the timing of crater formation remains unknown. The craters are aligned NW–SE (Fig. 4) and are distributed in a zone that is 500 m wide and 1,500 m long, suggesting that phreatic explosions during the past several thousand years have been confined to within this zone. The Hiyoriyama Cryptodome is also elongate NE–SW, indicating that ascending magma followed underground fractures with this orientation. We infer that the common alignment of the explosion craters and the cryptodome reflects the upwelling of magma and hydrothermal fluids along subsurface fractures with this orientation. The orientation of the fractures may reflect the tectonic stress field related to the northwestern movement of the Pacific Plate (see also Jackson *et al.*, 1975; Nakamura, 1977; Watanabe, 1993).

## 5. Conclusion

The Noboribetsu Geothermal Field formed as a result of complex ground deformation involving growth of the Hiyoriyama Cryptodome and formation of the Hiyoriyama Plain by river damming, and a number of explosion craters formed by phreatic eruptions. The common alignment of the explosion craters and the Hiyoriyama Cryptodome suggests the ascent of magma/fluid along

NW–SE-trending fractures. Three-dimensional laser-scanner surveys provide valuable geological information for understanding the geology of geothermal fields.

#### Acknowledgements

This research was sponsored by the Ministry of Education, Culture, Sports, Science and Technology of Japan (MEXT), and was supported financially by the Hokkaido Bureau of Economy, Trade and Industry (METI), and the Muroran Institute of Technology. We thank T. Nitta and M. Kiriki (Tanaka Consultant Co., Ltd) for assistance with the mapping survey, T. Chiba (Asia Air Survey Co., Ltd) for constructive suggestions in interpreting the map, N. Yabuki (Muroran Institute of Technology) for providing data on measurement accuracy, and A. Mogaki and Y. Oka (Muroran Institute of Technology) for help in the field. We are grateful to Y. Ishizaki (University of Toyama) and an anonymous referee for reviewing the manuscript. T. Watanabe (University of Toyama) is thanked for editing the manuscript.

#### References

- Chiba, T., Suzuki, Y. and Hiramatsu, T. (2007a) Digital terrain representation methods and red relief map, a new visualization approach. *J. Japan Cartographic Association (Map)*, **45**, 27–36 (in Japanese with English abstract).
- Chiba, T., Tomita, Y., Suzuki, Y., Arai, K., Fujii, N., Miyaji, N., Koizumi, S. and Nakashima, K. (2007b) Analysis of micro topography of the Aokigahara lava flows, Fuji volcano, by the light detection and ranging system. In *Fuji volcano* (Aramaiki, S., Fujii, T., Nakada, S. and Miyaji, N. eds.), 349–363, Yamanashi Institute of Environmental Sciences, Yamanashi, Japan (in Japanese).
- Goto, Y. and Danhara, T. (2011) Zircon fission-track dating of the Hiyoriyama Cryptodome at Kuttara Volcano, Hokkaido, Japan. *Bull. Volcanol. Soc. Japan*, **56**, 19–23.
- Goto, Y., Sasaki, H., Toriguchi, Y. and Hatakeyama, A. (2011) A phreatic explosion after AD1663 at the Hiyoriyama Cryptodome, Kuttara Volcano, southwestern Hokkaido, Japan. *Bull. Volcanol. Soc. Japan*, **56**, 147–152.
- Hunter, G., Pinkerton, H., Airey, P. and Calvari, S. (2003) The application of a long-range laser scanner for monitoring volcanic activity on Mount Etna. *J. Volcanol. Geotherm. Res.*, **123**, 203–210.
- Jackson, E.D., Show, H.R. and Barger, K.E. (1975) Calculated geochronology and stress field orientations along the Hawaiian chain. *Earth Planet. Sci. Lett.*, **26**, 145–155.
- Katsui, Y., Yokoyama, I., Okada, H., Abiko, T. and Muto, H. (1988) **Kuttara (Hiyoriyama), its volcanic geology, history of eruption, present state of activity and prevention of disasters**. Committee for Prevention and Disasters of Hokkaido, Sapporo, 99p (in Japanese).
- Machida, H. and Arai, F. (2003) **Atras of tephra in and around Japan**. University of Tokyo Press, Tokyo, 360p.
- Mimatsu, M. (1995) **Showa-shinzan diary**. Executive committee of the 50th anniversary of Mt. Showa-Shinzan, Sobetsu town, Hokkaido, 179p.
- Moriizumi, M. (1998) The growth history of the Kuttara volcanic group. *Bull. Volcanol. Soc. Japan*, **43**, 95–111 (in Japanese with English abstract).
- Moriya, I. (2003) Kuttara Volcano. In *Regional Geomorphology of the Japanese Islands, vol. 2, Geomorphology of Hokkaido* (Koaze T., Nogami, M., Ono, Y. and Hirakawa, K. eds.), 279–281, University of Tokyo Press, Tokyo (in Japanese).
- Nakamura, K. (1977) Volcanoes as possible indicators of tectonic stress orientation: Principle and proposal. *J. Volcanol. Geotherm. Res.*, **2**, 1–16.
- Pesci, A., Fabris, M., Conforti, D., Loddo, F., Baldi, P. and Anzidei, M. (2007) Integration of ground-based laser scanner and aerial digital photogrammetry for topographic modeling of Vesuvio volcano. *J. Volcanol. Geotherm. Res.*, **162**, 123–138.
- Watanabe, Y. (1993) Late Cenozoic stress field in northern part of southwest Hokkaido based on trends of dikes and craters. *Jour. Geol. Soc. Japan*, **99**, 105–116 (in Japanese with English abstract).
- Yamagata, K. (1994) Tephrochronological study on the Shikotsu and Kuttara Volcanoes in southwestern Hokkaido, Japan. *J. Geograph.*, **103**, 268–285 (in Japanese with English abstract).
- Yokoyama, I., Katsui, Y., Oba, Y. and Ehara, Y. (1973) **Usuzan, its volcanic geology, history of eruption, present state of activity and prevention of disasters**. Committee for Prevention and Disasters of Hokkaido, Sapporo, 254 p (in Japanese).
- Yokoyama, R., Sirasawa, M. and Kikuchi, Y. (1999) Representation of topographical features by openesses. *J. Japan Soc. Photogrammetry and Remote Sensing*, **38**, 26–34 (in Japanese with English abstract).

(Editorial handling Toru Watanabe)

## ヘリコプター搭載型高分解能レーザースキャナを用いた 北海道クッタラ火山登別地熱地域の3次元地形計測

後藤芳彦・松塚 悟・亀山聖二

ヘリコプター搭載型の高分解能レーザースキャナを用いて、北海道クッタラ火山、登別地熱地域の3次元地形計測を行った。計測範囲は登別地熱地域の全域を含む $2 \times 2.4 \text{ km}$ で、計測データから3次元デジタル地形図を作成した。その結果、登別地熱地域の詳細な火山地形が明らかになった。代表的な火山地形は、高粘性のマグマが貫入して形成された日和山潜在ドーム、日和山潜在ドームの隆起により川がせき止められてできた日和山平原、および北西-南東方向に配列する爆裂火口群である。日和山潜在ドームは北西-南東方向に伸長し、爆裂火口群も同方向に配列することから、地下深部のマグマおよび地熱流体は、北西-南東方向の割れ目に沿って上昇したと考えられる。高分解能レーザースキャナによる地形計測は火山地質の解明に極めて有効である。